Coherent Backscattering of Light by Cold Atoms

G. Labeyrie*, F. de Tomasi†, J.-C. Bernard*, C. A. Müller*, C. Miniatura* and R. Kaiser*

* Institut Non Linéaire de Nice, UMR 6618, 1361 route des Lucioles, F-06560 Valbonne.

† now at Dipartimento di Fisica, Universita di Lecce, via Arnesano.

(February 2, 2008)

Light propagating in an optically thick sample experiences multiple scattering. It is now known that interferences alter this propagation, leading to an enhanced backscattering, a manifestation of weak localization of light in such diffuse samples. This phenomenon has been extensively studied with classical scatterers. In this letter we report the first experimental evidence for coherent backscattering of light in a laser-cooled gas of Rubidium atoms.

Transport of waves in strongly scattering disordered media has received much attention during the past years when it was realized that interference can dramatically alter the normal diffusion process [1–3]. In a sample of randomly distributed scatterers, the initial direction of the wave is fully randomized by scattering and a diffusion picture seems an appropriate description of propagation when the sample thickness is larger than the scattering mean free path [4]. This model neglects all interference phenomena and predicts a transmission of the medium inversely proportional to sample thickness. This is the familiar Ohm's law. However, interferences may have dramatic consequences such as a vanishing diffusion constant [5]. In this situation, the medium behaves like an insulator (strong localization). Such a disorder induced transition has been reported for microwaves and for light [6]. In fact, even far from this insulating regime, interferences already hamper the diffusion process (weak localization). This has been demonstrated in coherent backscattering (CBS) experiments. Upon coherent illumination of a static sample, a random speckle pattern is generated. This pattern is washed out by configuration averaging except in a small angular range around the backscattering direction where constructive interferences originating from reciprocal light paths enhance diffuse reflection from the sample [7]. This effect has been observed for light in a variety of different media such as suspensions of powder samples, biological tissues or Saturn's rings [8], as well as for acoustic waves [9]. Among other interesting features such as universal conductance fluctuations [10] or lasing in random media [11], CBS is a hallmark of coherent multiple scattering.

Atoms as scatterers of light offer new perspectives. The achievements of laser cooling techniques [12,13] in the last decade now allow to manipulate and control samples of quantum scatterers. Cold atoms are unique candidates to move the field of coherent multiple scattering to a fully quantum regime (quantum internal structure, wave-particle duality, quantum statistical aspects). For instance, the coupling to vacuum fluctuations (spontaneous emission) is responsible for some unusual properties of the scattered light (elastic and inelastic spectra [14,15]). Also, information encoding in atomic internal states can erase interference fringes like in some "which-path" experiments [16]. Furthermore, it is now possible to implement situations where the wave nature of the atomic motion is essential [12,13].

In our experiment, the scattering medium is a laser-cooled gas of Rubidium atoms which constitutes a perfect monodisperse sample of strongly resonant scatterers of light. The quality factor of the transition used in our experiment is $Q = \nu_{at}/\Delta\nu_{at} \approx 10^8$ (D2 line at $\lambda = c/\nu_{at} = 780$ nm, intrinsic resonance width $\Delta\nu_{at} = \Gamma/2\pi = 6$ MHz). The scattering cross section can thus be changed by orders of magnitude by a slight detuning of the laser frequency ν_L. This is a new situation compared to the usual coherent multiple scattering experiments where resonant effects, if any, are washed out by the sample polydispersity. Moreover in our sample the duration τ_D (delay time) of a single scattering event largely dominates over the free propagation time between two successive scattering events : for on-resonant excitation ($\delta = \nu_L - \nu_{at} = 0$), this delay is of the order of $\tau_D \approx 2/\Gamma = 50$ ns corresponding to free propagation of light over 15 m in vacuum. In such a situation, particular care must be taken to observe a CBS effect. Indeed, when atoms move, additional phaseshifts are involved. Configuration averaging will only preserve constructive interference between reciprocal waves if the motion-induced optical path change Δx does not exceed one wavelength [17]. A rough estimate is $\Delta x = v_{rms}\tau_D < \lambda$, a criterium which can be written in the more appealing form $kv_{rms} < \Gamma$. Thus, for resonant excitation, the Doppler shift must be small compared to the width of the resonance. For Rubidium atoms illuminated by resonant light, one finds $v_{rms} < 4.6$ m/s corresponding to a temperature $T = 200$ mK. Much lower temperatures are easily achieved by laser cooling thus allowing observation of interference features in multiple scattering. However, up to now, only incoherent effects in multiple scattering, like radiation trapping [18], have been investigated in cold atomic vapors [19].

We prepare our atomic sample by loading a magneto-optical trap (MOT) from a dilute vapor of Rubidium 85

1

atoms [12] (magnetic gradient $\nabla B \approx 7\,\mathrm{G/cm}$, loading time $t_{load} \approx 0.7\,\mathrm{sec}$). Six independent trapping beams are obtained by splitting an initial laser beam slightly detuned to the red of the trapping transition (power per beam $30\,\mathrm{mW}$, FWHM diameter $2.8\,\mathrm{cm}$, Rubidium saturation intensity $I_{sat} \approx 1.6\,\mathrm{mW/cm^2}$, $\delta \approx -3\Gamma$). The repumper is obtained by two counterpropagating beams from a free running diode laser tuned to the $F = 3 \rightarrow F' = 3$ transition of the D2 line. Fluorescence measurements yield $N \approx 10^9$ atoms corresponding to a spatial density $n_{at} \approx 2 \times 10^9$ cm^{-3} at the center of the cloud (gaussian profile, FWHM diameter $\approx 7\,\mathrm{mm}$). The velocity distribution of the atoms in the trap has been measured by a time-of-flight technique to be $v_{rms} \approx 10\,\mathrm{cm/s}$, well below the limit imposed by the above velocity criterium. To observe coherent backscattering (CBS) of light, we alternate a CBS measurement phase with a MOT preparation phase. During the CBS phase, the magnetic gradient and trapping beams of the MOT are switched off (residual power per beam $0.2\,\mu\mathrm{W}$). The CBS probe beam (FWHM $\approx 6\,\mathrm{mm}$, spectral width $\Delta\nu_L \approx 1$ MHz) is resonant with the closed trapping transition of the D2 line : $F = 3 \rightarrow F' = 4$. A weak probe is used to avoid saturation effects (power $80\,\mu\mathrm{W}$, on-resonant saturation $s = 0.1$). The optical thickness of the sample, measured by transmission, is $\eta \approx 4$ and remains constant, within a few percent, during the whole duration of the CBS measurement phase ($2.5\,\mathrm{ms}$). The corresponding extinction mean free path $\ell \approx 2\,\mathrm{mm}$ is consistent with an estimation deduced from our fluorescence measurements, taking a scattering cross-section at resonance $\sigma_{res} = 3\lambda^2/2\pi$.
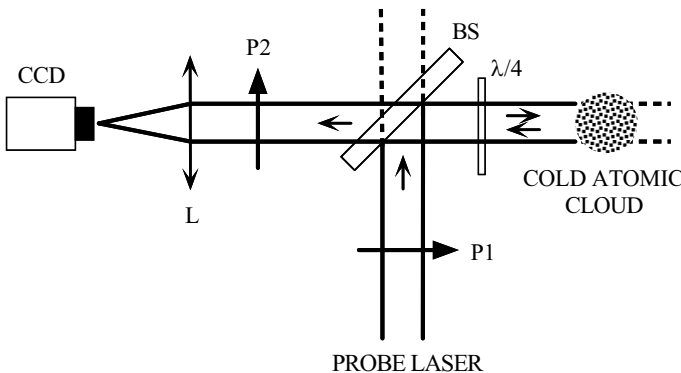

FIG. 1. The CBS detection scheme. P1, P2 : polarizers; $\lambda/4$: quarter-wave plate; BS : beam-splitter (T = 90%); L : analysis lens ($f = 500$ mm).

The CBS detection setup is shown in Fig.1. It involves a cooled CCD camera in the focal plane of a converging lens ($f = 500$ mm). A polarization sensitive detection scheme, generally allowing to eliminate the single scattering contribution [20], is used for signal recording in various polarization channels. For a linear incident polarization, we record the scattered light with (linear)

polarization parallel ("parallel" channel) or orthogonal ("orthogonal" channel) to the incident one. We also use a circular incident polarization by inserting a quarter-wave plate between the beam-splitter and the sample. In the "helicity preserving" channel the detected polarization is circular with the same helicity (sign of rotation of the electric field referenced to the wave propagation direction) as the incident one : as an example, no light is detected in this channel in the case of the back-reflection by a mirror. This is the channel mostly used in previous studies, because it allows to eliminate the single scattering contribution (for dipole-type scatterers). The "helicity non-preserving" channel is obtained for a detected circular polarization orthogonal to the previous one. Teflon or dilute milk samples were used to find the exact backward direction, to cross-check the polarization channels and to test the angular resolution of our set-up. During the MOT phase (duration $10\,\mathrm{ms}$), probe beam and detection scheme are switched off while the MOT is switched on again to recapture the atoms. After this phase a new atomic sample is reproduced. The whole sequence is repeated for a typical duration of 1 min with a detected flux typically about 1800 photons/pixel/sec. A "background" image, representing less than 10% of the full signal level (due mainly to scattering from the repumper by hot atoms in the cell), is substracted from the "CBS" image to suppress stray light contributions.

FIG. 2.

Fig. 2 (color image in appendice) shows the CBS images obtained from our laser-cooled Rubidium vapor in the various polarization channels. We clearly observe enhanced backscattering in all four polarization channels whereas for a thick teflon sample we only found pronounced cones in the polarization preserving channels. This enforces the idea that low scattering orders are dominant in our experiment [21] which is not surprising considering the relatively small optical thickness of our sample. The intensity enhancement factors, defined as the ratio between the averaged intensity scattered in exactly backward direction and the large angle background are 1.11, 1.06, 1.08 and 1.09 for the helicity preserving, helicity non-preserving, orthogonal and parallel channels respectively. The detected light intensities in these channels, normalized to that of the linear parallel channel, are 0.76, 0.77, 0.54 and 1. A closer look at Fig.2d reveals that the cone exhibits a marked anisotropy in the (linear) parallel polarization channel: the cone is found to broader in the (angular) direction parallel to the incident polarization. This effect has already been observed in classical scattering samples and is also a signature of low scattering orders [21].

For a more quantitative analysis of the CBS cone, we report in Fig.3 a section of image 2a (helicity non-preserving channel), taken after an angular average was

performed on the data (this procedure is justified when the cone is isotropic, as in Fig.2a). The measured cone width $\Delta\theta$ is about 0.57 mrad, nearly six times larger than our experimental resolution of 0.1 mrad. Taking into account the experimental resolution, we compared our data to a calculation (dotted line) involving only double scattering [7]. The experimental value $\ell \approx 2$ mm for the mean free path was used in the calculation, leaving the enhancement factor as free parameter. Even though the assumptions underlying this theoretical model (isotropic double scattering, semi-infinite medium) are rather crude in our case, the shape of the CBS cone is nicely reproduced. We plan, in further studies, to investigate in more details the contributions of different scattering orders by carefully analyzing the CBS cone shape.
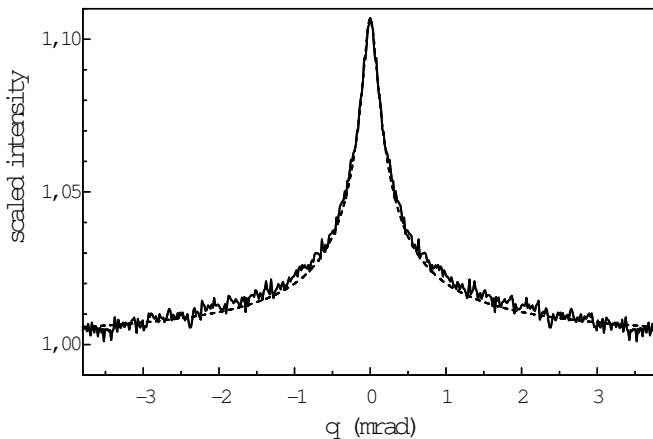

FIG. 3. Atomic CBS cone in the helicity non-preserving channel. The experimental profile (solid line) is a section of the 2D image of Fig. 2a (after angular averaging). The dashed curve is a fit by a model assuming only double scattering, with the mean free path determined experimentally and the enhancement factor the only adjustable parameter.

One important aspect in CBS studies has always been the enhancement factor in the backscattering direction, due to the constructive interferences between reciprocal paths. In the helicity preserving channel, this enhancement factor is known to be 2 for independent scattering by classical scatterers [8], as single scattering can be ruled out in that polarization channel. In our experiment with cold atoms however, we measure a backscattered enhancement of 1.06, clearly less than 2 ! This reduction cannot be attributed to the experimental resolution, as we have measured enhancement factors on milk (using a dilution giving the same cone width as the atomic one) of 1.8. However, in our situation several processes could reduce the cone contrast. The first one is single scattering, which does not contribute to CBS. Due to the presence of several Zeeman sublevels in the groundstate of Rubidium

atoms, Raman processes, i.e. light scattering with change of the atomic internal sublevel, have to be considered. In such events, the polarization of the scattered light differs from the incident polarization and single scattering is not eliminated even in the helicity preserving channel. Another consequence of the atom's internal structure is a possible imbalance between the amplitudes of the reciprocal waves : atoms in different internal states can have different scattering cross sections (resulting from different Clebsch-Gordan coefficients). They can thus be seen as partial polarizers which can imbalance the amplitude of the paths which interfere for CBS. Furthermore finite-size effects should also be taken into account. Indeed our sample does not have the standard slab geometry and the gaussian shape of the probe beam is known to reduce the enhancement factor. We are currently investigating these effects to determine their respective magnitudes for our situation. Also, some more subtle phenomena might play an additional role in the cone reduction. For instance, with classical scatterers, the radiated and the incident light have identical frequencies (elastic scattering). This is no longer true for atoms for which the resonant fluorescence spectrum displays inelastic structures in addition to the usual elastic component [14,15]. Because of Raman scattering, even in the weak saturation limit (weak probe intensity), atoms have a non-negligible probability to undergo inelastic scattering [15]. The role of these rather complex spectral properties in coherent backscattering has yet to be studied both theoretically and experimentally.

In summary we have reported the first observation of coherent backscattering of light by a sample of laser cooled atoms. These first results indicate that in our system low scattering orders are dominant, as expected from optical thickness measurements. The exact value of the enhancement factor and the precise shape of the cone is not yet fully understood and requires more experimental and theoretical investigations. Further experiments will include studies of the effect of the probe beam intensity (which determines the amount of inelastic scattering) and detuning. Detuning the laser frequency from the atomic resonance leads to an increased mean free path $\ell = 1/n_{at}\sigma$. Indeed, we already observed that the measured width $\Delta\theta$ of the coherent backscattering cone decreases when the probe frequency is detuned from resonance, as expected from the scaling $\Delta\theta \propto \lambda/\ell$ [7]. It would be very interesting to extend these experiments to new regimes. Weak and strong localization of light in gaseous Bose-Einstein condensates and of atomic matter waves in random optical potentials certainly present a great challenge for the near future.

[1] Sharvin, D.Yu., & Sharvin,Yu.V., JETP Lett. **34**, 272-275 (1981).

[2] Scattering and Localization of Classical Waves in Random Media, P. Sheng, Eds. (World Scientific, Singapore, 1990).

[3] Mesoscopic Quantum Physics, E. Akkermans, G. Montambaux, J.-L. Pichard & J. Zinn-Justin, Eds., Elsevier Science B.V. (North Holland, Amsterdam, 1995).

[4] Chandrasekhar, S., Radiative transfer (Dover, New York, 1960).

[5] Anderson, P.W., Phys. Rev. **109**, 1492-1505 (1958).

[6] Wiersma, D.S., Bartolini, P., Lagendijk, A. & Righini, R. Nature **390**, 671-673 (1997); Gresillon, S., et al., Phys. Rev. Lett. **82**, 4520-4523 (1999); Genack, A.Z. & Garcia, N., Phys. Rev. Lett. **66**, 2064-2067 (1991).

[7] van Tiggelen, B.A., Lagendijk, A. & Tip, A., J. Phys.: Condens. Matter **2**, 7653-7677 (1990).

[8] Wiersma, D.S., van Albada, M.P., van Tiggelen, B.A. & Lagendijk, A., Phy. Rev. Lett. **74**, 4193-4196 (1995); Yoo, K.M., Tang, G.C. & Alfano, R.R., Appl. Opt. **29**, 3237-3239 (1990); Mishchenko, M.I., Astrophys. J. **411**, 351-361 (1993).

[9] Tourin, A., Derode, A., Roux, P., van Tigelen, B.A. & Fink, M., Phys. Rev. Lett. **79**, 3637-3639 (1997).

[10] Scheffold, F. & Maret, G. Phys. Rev. Lett. **81**, 5800-5803 (1998).

[11] Cao, H., et al., Phys. Rev. Lett. **82**, 2278-2281 (1999).

[12] Laser Manipulation of Atoms and Ions, E. Arimondo, W.D. Phillips & F. Strumia, Eds. (North Holland, Amsterdam, 1992).

[13] Anderson, M.H., Ensher, J.R., Matthews, M.R., Wieman, C.E. & Cornell, E.A., Science **269**, 198-201 (1995). Davis, K.B., et al., Phys. Rev. Lett. **75**, 3969-3973 (1995).

[14] Mollow, B.R., Phys. Rev. **188**, 1969-1975 (1969).

[15] Gao, B., Phys. Rev. A **50**, 4139-4156 (1994).

[16] Itano, W.M., et al., Phys. Rev. A **57**, 4176-4187 (1998).

[17] Golubentsev, A.A., Sov. Phys. JETP **59**, 26-34 (1984).

[18] Holstein, T., Phys. Rev. **72**, 1212-1233 (1947).

[19] Fioretti, A., Molisch, A.F., Muller, J.H., Verkerk, P. & Allegrini, M., Optics Comm. **149**, 415-422 (1998).

[20] van Albada, M.P. & Lagendijk, A., Phys. Rev. Lett. **55**, 2692-2695 (1985); Wolf, P.-E. & Maret, G., Phys. Rev. Lett. **55**, 2696-2699 (1985).

[21] van Albada, M.P., van der Mark, M. & Lagendijk, A., Phys. Rev. Lett. **58**, 361-364 (1987).

This figure "fig2.gif" is available in "gif" format from:

http://arXiv.org/ps/physics/9911010v1